STM JOURNALS

Journal of
Polymer & Composites

ISSN: 2321-2810 (Online)
ISSN: 2321-8525 (Print)
Volume 13, Issue 2, 2025
DOI (Journal): 10.37591/JoPC

https://journals.stmjournals.com/JOPC/

Research JoPC

Comparison of 11-Atom Armchair Graphene Nanoribbons and Zig-Zag Carbon Nanotubes in Polymer Composites Under Various Bias Voltages: A Study of Electronic and Transmission Properties

Anabathula Udaya Sri[1,*], D. Vinay Kumar[2]

Abstract

In this research, 11-atom zig-zag carbon nanotubes (ZCNTs) and 11-atom armchair graphene nanoribbons (AGNRs) were studied under applied bias voltages at 50, 150, and 300 millivolt levels. The focus was on understanding their behaviour concerning transmission qualities, current-voltage (I-V) characteristics, and energy-momentum (E-K) diagrams. The Non-Equilibrium Green's Function (NEGF) approach was employed to analyse various electronic properties for ZCNTs and AGNRs, including transmission, E-K relationships, and I-V characteristics. The results show that for the same number of atoms and material, the bandgap of AGNRs is lower than that of ZCNTs, associated with an increased probability of electron transmission in a constrained energy range. When integrated into polymer composites, the wider ribbon widths of AGNRs compared to ZCNTs enhance electrical conductivity within the polymer matrix. AGNRs' I-V characteristics exhibit linear behaviour under a 50-mV bias, whereas at 150 and 300 mV, a plateau in current flow is observed after reaching a peak voltage. Conversely, ZCNTs display non-linear behaviour, with current flow decreasing after reaching a peak at 300 mV. These differences are attributed to the robust electron-electron bonds and the effects of quantum confinement, which can influence the performance of graphene- or nanotube-reinforced polymer nanocomposites in electronic applications. This study provides valuable insights into the electrical characteristics of AGNRs and ZCNTs, offering promising opportunities for their integration into polymer-based nanoelectronics composites for applications in flexible electronics, electromagnetic shielding, and energy storage systems.

Keywords: AGNRs, ZCNTs, polymer nanocomposites, current-voltage characteristics, energy-momentum

***Author for Correspondence**
Anabathula Udaya Sri
E-mail: udayasrivfstr@gmail.com

[1]Research Scholar, Department of Mechanical Engineering, Vignan's Foundation for Science Technology and Research, Vadlamudi, Andhra Pradesh, India
[2]Associate Professor, Department of Mechanical Engineering, Vignan's Foundation for Science Technology and Research, Vadlamudi, Andhra Pradesh, India

Received Date: October 05, 2024
Accepted Date: January 13, 2025
Published Date: January 23, 2025

Citation: Anabathula Udaya Sri, D. Vinay Kumar. Comparison of 11-Atom Armchair Graphene Nanoribbons and Zig-Zag Carbon Nanotubes in Polymer Composites Under Various Bias Voltages: A Study of Electronic and Transmission Properties. Journal of Polymer & Composites. 2025; 13 (2): 126–134p.

INTRODUCTION

In the realm of advanced nano-electronic devices, Graphene Nanoribbons (GNRs) have emerged as a subject of intense interest due to their exceptional mechanical, electrical, and thermal properties [14]. Among the different types of GNRs, Armchair Graphene Nanoribbons (AGNRs) stand out for their superior electronic features, such as tunable bandgap and high carrier mobility, ideal candidates for nano electronic applications. While much research has focused on the transport properties of AGNRs using various theoretical approaches, a comprehensive understanding of their behavior under non-equilibrium conditions, particularly in response to bias voltage, remains elusive. Previous

studies have demonstrated that edge states and the distinctive bandgap of AGNRs significantly influence their electrical characteristics [1]. The bandgap of AGNRs can be tailored by altering the ribbon's width and edge structure, enhancing their utility in applications requiring precise electronic properties [2-4]. Additionally, the electronic properties of AGNRs are sensitive to the presence of defects, which can modify charge transport and conductivity [5-7]. Despite this, the impact of defects on AGNR transport properties under biased voltage conditions remains underexplored.

This method has been used to investigate various electronic characteristics in nanoscale systems, including transmission, energy-momentum (E-K) diagrams, current-voltage (I-V) characteristics, and noise properties. Moreover, it is valuable in exploring how factors such as disorder and other variables impact the electronic properties of the system.

The NEGF method is widely used in various nanoscale structures, including semiconductor quantum dots, graphene nanoribbons, and carbon nanotubes. It is an effective tool for investigating the transport properties of complex systems.

In this research, the investigation focused on how 11-atom armchair graphene nanoribbons (AGNRs) and Zig-zag Carbon Nanotubes (ZCNTs) react to applied bias voltages of 50 millivolts, 150 millivolts, and 300 millivolts. The main objective was to gain a good understanding of their behavior concerning energy-momentum (E-K) diagrams, current-voltage (I-V) characteristics, and transmission properties. It is important to carefully examine the various electronic characteristics of ZCNTs and AGNRs, for which the Non-Equilibrium Green's Function method was used, providing insights into factors such as transmission, E-K relationships, and I-V characteristics [20-22].

METHODOLOGY

To study the I-V characteristics and transmission of Armchair Graphene Nano Ribbons (AGNRs) and Zigzag Carbon Nanotubes (ZCNTs) using the Non-Equilibrium Green's Function method, a model is created with a tight-binding Hamiltonian considering carbon atom interactions within the honeycomb lattice [23]. This model establishes a scattering region with AGNRs and ZCNTs connected to semi-infinite leads representing source and drain electrodes, assuming that both leads are made of the same material as the channel. Bias voltages are applied to the leads to create a non-equilibrium state, and Green's functions are calculated to describe electron propagation. The analysis includes determining transmission coefficients and I-V characteristics to understand electron transmission and current flow through the system, leading to insights into the electronic properties of AGNRs and ZCNTs under biased conditions.

The subsequent step involves formulating the Non-Equilibrium Green's Function (NEGF) equations. These equations are derived by integrating the Hamiltonian with self-energy functions that describe the connection between the scattering region (comprising AGNRs and ZCNTs) and the leads (representing the source and drain electrodes). These self-energy functions play a crucial role in elucidating the coupling of AGNRs and ZCNTs to the electrodes. Subsequently, the NEGF equations are solved using numerical methods, specifically employing the iterative Green's function technique. This methodology enables the determination of the transmission properties and I-V characteristics of AGNRs and ZCNTs [20-24].

In the third step, the accuracy and reliability of the NEGF method are evaluated by comparing its results with data obtained from other theoretical approaches. This comparative analysis serves to validate the findings and ascertain the method's efficacy in predicting electronic properties.

The final step involves investigating how different factors impact the electronic properties of AGNRs and ZCNTs when subjected to bias voltages of 50 millivolts, 150 millivolts, and 300 millivolts. These factors include the width, length, bias voltage, temperature, and doping level of AGNRs and ZCNTs. However, the primary focus of this paper remains on their behavior regarding transmission properties, Energy-Momentum (E-K) relationships, and current-voltage (I-V) characteristics. The NEGF method

is used to thoroughly analyze various electronic attributes of both AGNRs and ZCNTs, allowing for an exploration of aspects such as transmission, E-K relationships, and I-V characteristics.

Additionally, the expression for the calculation of the quantum wave function (Ψ) for any type of particle, such as an electron, can be derived from the Schrödinger equation

$$i\hbar\frac{\partial}{\partial t}\Psi(r,t)=\left[\frac{-\hbar^2}{2m}\nabla^2+V(r,t)\right]\Psi(r,t) \tag{1}$$

Expression for the calculation of quantum wave (Ψ) for Time Independent particle (Time Independent Schrodinger Equation)

$$\left[\frac{-\hbar^2}{2m}\nabla^2+V(r)\right]\Psi(r)=E\Psi(r) \tag{2}$$

Expression for the calculation of quantum wave (Ψ) for free electrons

$$\frac{-\hbar^2}{2m}\nabla^2\Psi(r)=E\Psi(r) \tag{3}$$

By solving the above-obtained equation here the function

$$\Psi=A\cos\left(\frac{2\pi}{\lambda}x\right) \tag{4}$$

Expression for Green's Function

$$\mathrm{G(E)}=(\mathrm{EI}-\mathrm{H}-\Sigma_{\mathrm{L}}-\Sigma_{\mathrm{R}})^{-1} \tag{5}$$

Channel current-calculation Expression

$$\mathrm{I_{LR}}=\int_{-\infty}^{\infty}\frac{\mathrm{e}}{h}\mathrm{T(E)}(\mathrm{f_L}-\mathrm{f_R})\mathrm{dE} \tag{6}$$

Fermi-level energy Expression

$$\mathrm{f}=\frac{1}{1+\mathrm{e}^{\frac{\mathrm{E}-\mathrm{E_F}}{\mathrm{kT}}}} \tag{7}$$

Expression for propertyof transmission

$$\mathrm{T(E)}=\mathrm{tran}(\Gamma_{\mathrm{L}}\mathrm{G(E)}\Gamma_{\mathrm{R}}\mathrm{G^*(E)}) \tag{8}$$

Expression of Green's Function

$$\mathrm{G(E)}=(\mathrm{EI}-\mathrm{H}-\Sigma_{\mathrm{L}}-\Sigma_{\mathrm{R}})^{-1} \tag{9}$$

Self-energy Expression

$$\Sigma=\tau g\tau^{+} \tag{10}$$

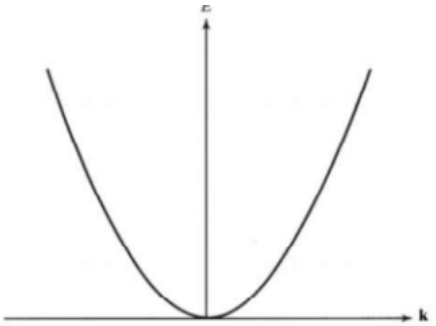

Figure 1. E-K diagram for free electron.

E = energy of an electron, K = wave vector, for free electron the Potential Energy is zero

K.E + P.E = T.E, Hence K.E = T.E

$$E = \frac{h^2 k^2}{2m} \tag{11}$$

Figure 1 illustrates the relationship between electron energy and velocity as the wave vector (K) of free electrons ranges from "0" to "∞." This transition in wave vector corresponds to a shift in energy (E) from "0" to "∞." This graphical representation is commonly referred to as the Energy-Momentum (E-K) diagram, which is a valuable tool for understanding the permissible energy levels and associated momentum of electrons at specific energy states. The E-K diagram also provides information about a material's structural characteristics, indicating whether it behaves like a semiconductor or a metal and whether its band gap is direct or indirect [18-22]. While one approach to determining the band, gap involves extracting it directly from the E-K diagram, it can also be determined by analyzing the material's electronic characteristics, often through the simplification of the time-independent equation, leading to valuable insights.

$$H\Psi = E\Psi \tag{12}$$

where H=Hamiltonian operator (energy operator) and E=Energy eigenvalue.

RESULTS AND DISCUSSION

The study used the NEGF approach to analyze the electrical properties of ZCNTs and AGNRs under different bias voltages. Results showed that AGNRs have broader ribbon widths and narrower bandgaps than ZCNTs, indicating lower energy requirements for electron movement. Both AGNRs and ZCNTs exhibited high transmission coefficients, suggesting good conductivity. At higher bias voltages, AGNRs showed a constant current, while ZCNTs exhibited a decrease, attributed to electron interactions and quantum effects. These findings enhance our understanding of these materials for potential nanoelectronics applications.

Figure 2 depicts the atomic arrangement of both 11-atom AGNR and ZCNT under a honeycomb configuration. The AGNR exhibits a width of 1.23 nm, whereas the ZCNT has a width of 0.43 nm. Comparing both materials with the same number of atoms reveals an interesting fact: the ribbon width of armchair graphene nanoribbons (AGNRs) is significantly larger than that of zigzag carbon nanotubes (ZCNTs). This difference in width is a result of the different structures of AGNRs and ZCNTs. AGNRs have a flat, ribbon-like structure with edges that consist entirely of carbon atoms, while ZCNTs have a cylindrical structure with a zigzag pattern along the circumference. The larger width of AGNRs makes them more suitable for certain applications where a wider structure is desired, while the narrower width of ZCNTs may be advantageous in applications requiring a more compact structure.

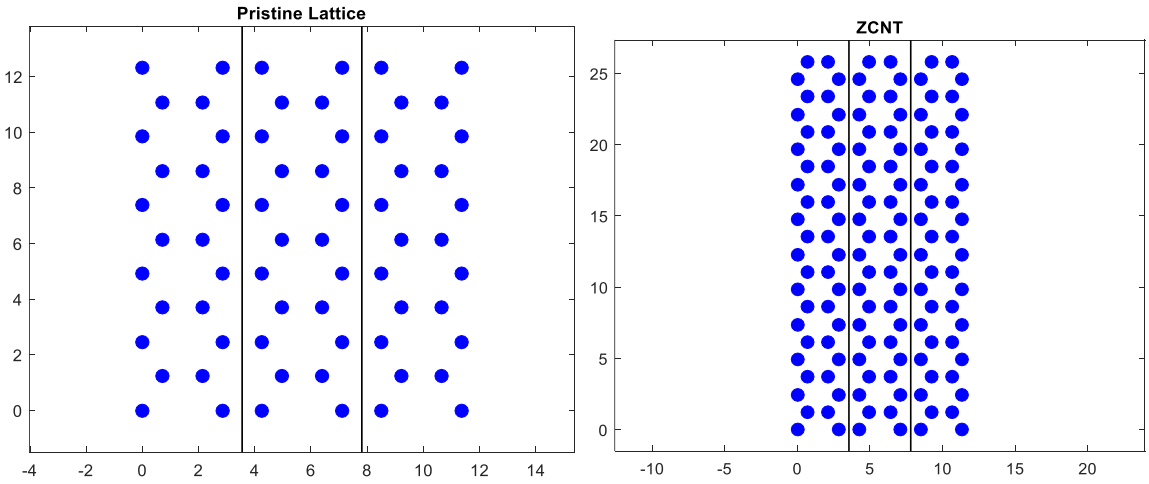

Figure 2. Pristine lattice of 11-AGNR and ZCNT honeycomb structure.

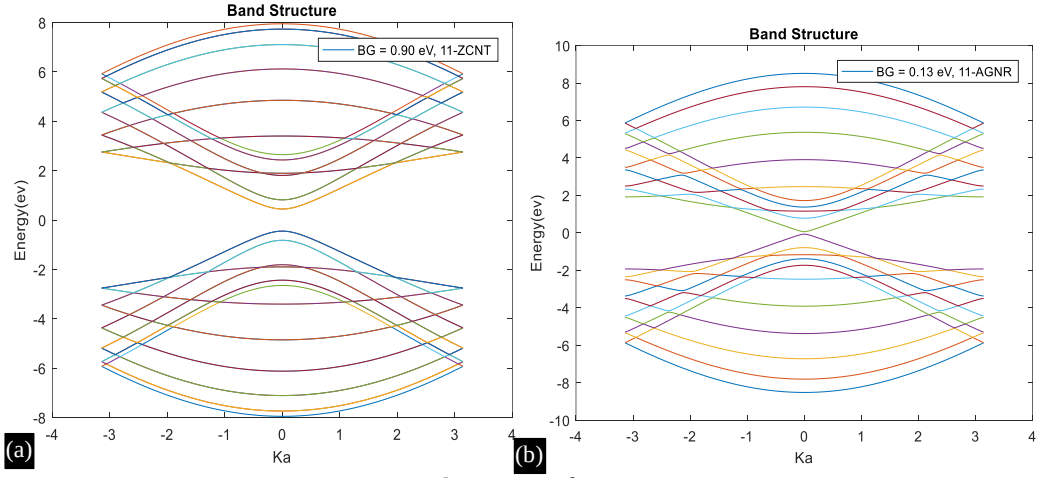

Figure 3. Energy-momentum (E-K) diagrams of11-atom AGNR&ZCNT (a) 11-AGNR, (b) 11-ZCNT.

Figure 3 illustrates the band structure of 11-atom AGNRs and ZCNTs with armchair edges in an Energy-Momentum (E-K) diagram. The diagram shows two distinct bands separated by a band gap. The upper set of bands represents the conduction bands, which are not fully occupied by electrons, while the lower set represents the valence bands, which are completely occupied by electrons. The obtained band gap values are 0.13 eV for 11-atom AGNRs and 0.90 eV for ZCNTs. This band gap indicates the energy required to transmit an electron from the valence band to the conduction band, and it has a significant impact on the electrical characteristics of ZCNTs and AGNRs.

The band structure of 11-atom AGNRs and ZCNTs with armchair edges demonstrates a substantial band gap, which arises due to quantum confinement effects. This study reveals that when comparing materials with the same number of atoms, the band gap in AGNRs is significantly narrower than that of ZCNTs. This difference implies that the energy required for electron transmission from the valence band to the conduction band is lower in AGNRs than in ZCNTs.

Figure 4. illustrates the Transmission-Energy diagram, providing valuable data on the electronic properties of 11-atom ZCNTs and 11-atom AGNRs over an energy range from -12 eV to +12 eV. The specific shape of the diagram is influenced by various factors of AGNRs and ZCNTs, including their dimensions, doping levels, and temperature. The relationship between energy and momentum in the transmission-energy diagram shows nonlinearity within this energy range.

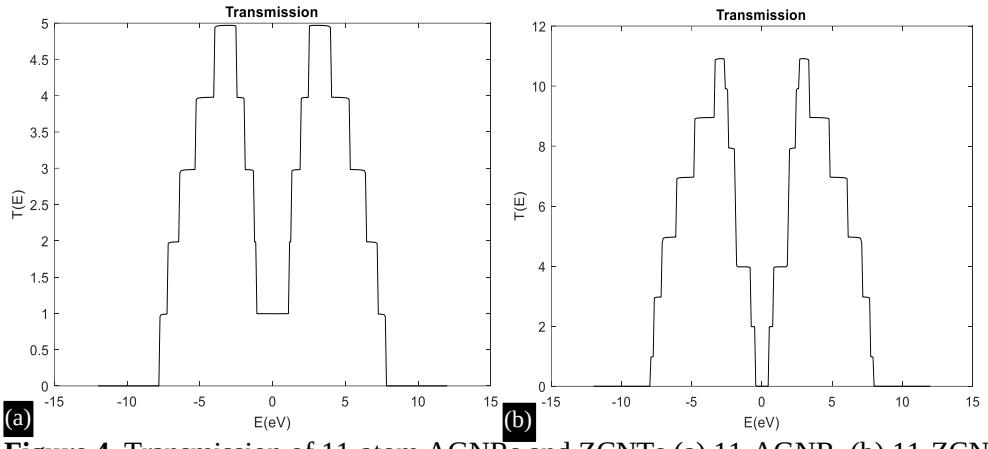

Figure 4. Transmission of 11-atom AGNRs and ZCNTs (a) 11-AGNR, (b) 11-ZCNT.

This nonlinearity is attributed to eigenvalues that create an electric field inside the ZCNT and AGNR, leading to changes in the energy levels of the holes and electrons in the structure. Importantly, this phenomenon is associated with the narrower band gap in AGNRs compared to ZCNTs, indicating that AGNRs require less energy to move an electron from the valence band to the conduction band than ZCNTs.

Figure 5 illustrates the current passing through both AGNRs and ZCNTs under a bias voltage of 50 mV. As the voltage is applied, the current through both structures increases from zero. The current-voltage characteristics of AGNRs exhibit a linear behavior under 50 millivolts, reaching a saturation point where the current levels off. This saturation current is limited by the available number of conducting states in AGNRs. In contrast, ZCNTs display a different behavior, with a decrease in current after reaching the saturation point in the I-V curve. The I-V trends in Figure 5 indicate a larger carrier concentration, as evidenced by a steeper I-V curve and a higher saturation current.

Figure 6 illustrates the current-voltage behavior of 11-atom AGNRs and 11-atom ZCNTs under a 150-mV bias voltage. As the voltage is applied, both AGNRs and ZCNTs exhibit a rapid increase in current from zero. These specific AGNRs and ZCNTs show linear current-voltage (I-V) characteristics initially when subjected to a 150-millivolt bias, ultimately attainment a saturation point wherever the current stabilizes. The saturation current is primarily determined by the available conducting states within AGNRs and ZCNTs.

However, beyond this saturation point, AGNRs maintain a constant current, while ZCNTs show a decrease in current in the I-V curve. This pattern can be attributed to a greater carrier concentration and the possibility of a band gap in the structures of AGNRs and ZCNTs. It also relates to the steeper I-V curve and higher saturation current noted in both sets of I-V plots.

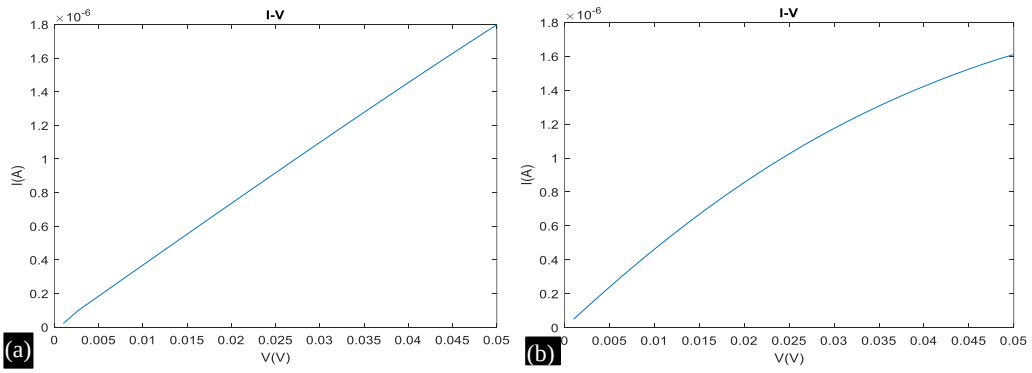

Figure 5. I-V Characteristics of 11-atom AGNRs under bias voltage of 50mV (a) 11-AGNR, (b) 11-ZCNT.

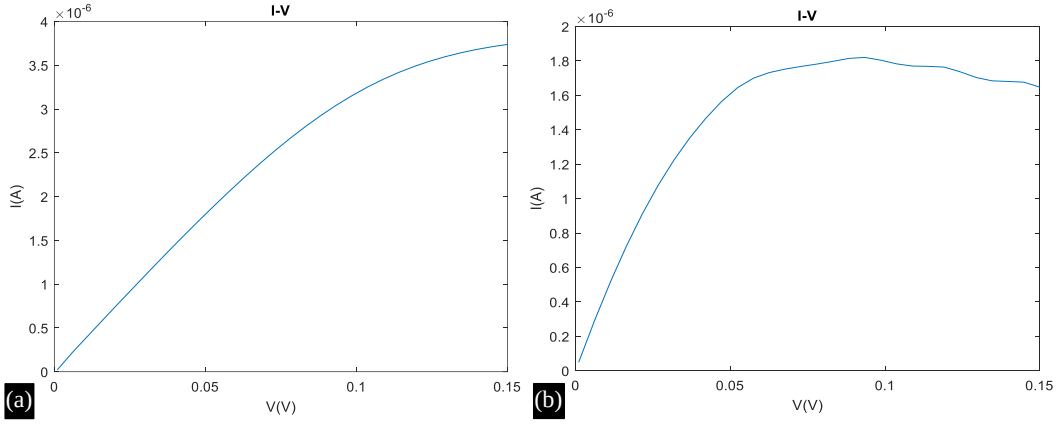

Figure 6. I-V Characteristics of 11-atom AGNRs and ZCNTs under a bias voltage of 150mV (a) 11-AGNR, (b) 11-ZCNT.

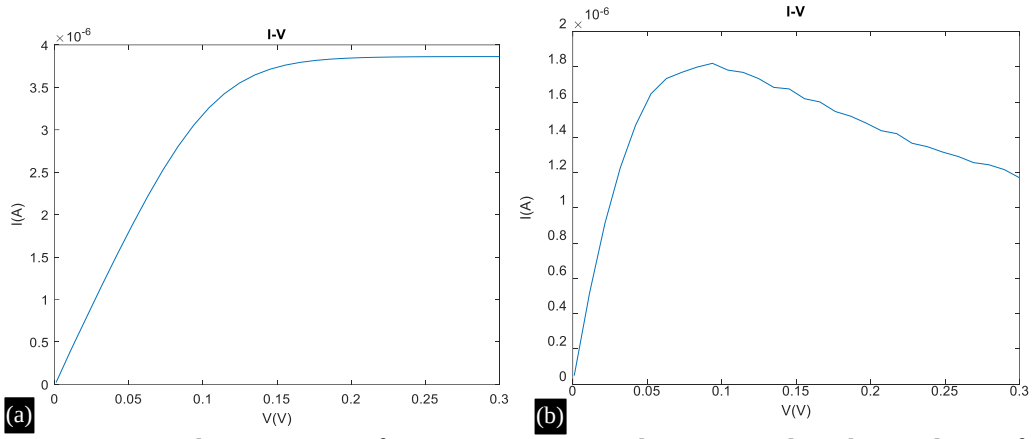

Figure 7. I-V Characteristics of 11-atom AGNRs and ZCNTs under a bias voltage of 300mV (a) 11-AGNR, (b) 11-ZCNT.

Figure 7 depicts the current behavior in 11-atom AGNRs and 11-atom ZCNTs under a bias voltage of 300mV. As the voltage is applied, the current initially increases from zero for both the 11-atom AGNR and ZCNT. These specific AGNRs and ZCNTs exhibit linear current-voltage (I-V) characteristics when subjected to a 300-millivolt bias, reaching a saturation point where the current stabilizes. The available conducting states within the AGNRs and ZCNTs primarily determine the saturation current.

After reaching this saturation point, AGNRs maintain a constant current, while ZCNTs exhibit a further decrease in current or a reduction in the I-V curve. This behavior corresponds to the steeper I-V curve and greater saturation current observed in both sets of I-V graphs shown in Figure 7, and is explained by the presence of a band gap and higher carrier concentration in the structures of ZCNTs and AGNRs.

CONCLUSIONS

In this paper, research has been conducted to investigate the transmission, Energy-Momentum (E-K) diagrams, and I-V characteristics of ZCNTs and 11-atom AGNRs under three different bias voltages (50 mV, 150 mV, and 300 mV) using the NEGF approach. The study has yielded significant insights into the behavior of AGNRs and ZCNTs. An interesting observation is that AGNRs have significantly broader ribbon widths than ZCNTs, and AGNRs also display narrower bandgaps than ZCNTs, indicating that AGNRs require less energy for electron movement between valence and conduction bands compared to ZCNTs.

Additionally, the study has revealed that both AGNRs and ZCNTs exhibit higher transmission coefficients for the same number of atoms within the energy range of -12 mV to +12 mV, peaking at the Fermi energy, indicating good conductivity of AGNRs and ZCNTs. Regarding the I-V characteristics, different behaviors were observed at different bias voltages. Both 11-atom AGNRs and ZCNTs show linear responses at a 50-millivolt bias, while at higher bias voltages of 150 and 300 millivolts, they exhibit uniform current flow after reaching a peak voltage. In contrast, ZCNTs display distinct non-linear behavior that becomes more pronounced with increasing voltage, with a noticeable decrease in current after reaching the peak voltage at 300 millivolts. These differences in behavior can be attributed to robust electron-electron bonds and quantum confinement effects.

This study demonstrates the NEGF's effectiveness in analyzing AGNRs' and ZCNTs' electrical properties, offering insights for future electronic device design. Further research is crucial for a comprehensive understanding.

REFERENCES

1. Kadonoff, L., and G. Byam. "Quantum Statistical Mechanics: Green's Function Method in Equilibrium and Nonequilibrium Problems." (1989).
2. Meir, Yigal, and Ned S. Wingreen. "Landauer formula for the current through an interacting electron region." *Physical review letters* 68.16 (1992): 2512.
3. Szałowski, Karol. "Graphene nanoflakes in external electric and magnetic in-plane fields." *Journal of Magnetism and Magnetic Materials* 382 (2015): 318-327.
4. Cai, Jinming, et al. "Atomically precise bottom-up fabrication of graphene nanoribbons." *Nature* 466.7305 (2010): 470-473.
5. Sadeghi, Mir Mohammad, Michael Thompson Pettes, and Li Shi. "Thermal transport in graphene." *Solid State Communications* 152.15 (2012): 1321-1330.
6. Yin, Yiheng, et al. "Tellurium nanowire gate-all-around MOSFETs for sub-5 nm applications." *ACS Applied Materials & Interfaces* 13.2 (2021): 3387-3396.
7. Zhou, Min, Hao Jin, and Yanxia Xing. "In-plane dual-gated spin-valve device based on the zigzag graphene nanoribbon." *Physical Review Applied* 13.4 (2020): 044006.
8. Son, Young-Woo, Marvin L. Cohen, and Steven G. Louie. "Energy gaps in graphene nanoribbons." *Physical review letters* 97.21 (2006): 216803.
9. Wakabayashi, Katsunori, et al. "Edge effect on electronic transport properties of graphene nanoribbons and presence of perfectly conducting channel." *Carbon* 47.1 (2009): 124-137.
10. Li, Xiaolin, et al. "Chemically derived, ultrasmooth graphene nanoribbon semiconductors." *science* 319.5867 (2008): 1229-1232.
11. Yang, Siqi, et al. "First-principles study of zigzag MoS2 nanoribbon as a promising cathode material for rechargeable Mg batteries." *The Journal of Physical Chemistry C* 116.1 (2012): 1307-1312.
12. Kim, Hee Jin, et al. "Recent advances in non-precious group metal-based catalysts for water electrolysis and beyond." *Journal of Materials Chemistry A* 10.1 (2022): 50-88.
13. Wu, Qingyun, et al. "Electronic and transport properties of phosphorene nanoribbons." *Physical Review B* 92.3 (2015): 035436.
14. Wakabayashi, Katsunori, et al. "Electronic transport properties of graphene nanoribbons." *New Journal of Physics* 11.9 (2009): 095016.
15. Li, Dongde, et al. "The spin-dependent electronic transport properties of M (dcdmp) 2 (M= Cu, Au, Co, Ni) molecular devices based on zigzag graphene nanoribbon electrodes." *Physics Letters A* 382.21 (2018): 1401-1408.
16. Zhang, Peina, et al. "π-magnetism and spin-dependent transport in boron pair doped armchair graphene nanoribbons." *Applied Physics Letters* 120.13 (2022).
17. Liu, Lizhao, et al. "Electromechanical properties of zigzag-shaped carbon nanotubes." *Physical Chemistry Chemical Physics* 15.40 (2013): 17134-17141.

18. Suzuki, Satoru, ed. *Syntheses and applications of carbon nanotubes and their composites*. BoD–Books on Demand, 2013.
19. Dresselhaus, G., Mildred S. Dresselhaus, and Riichiro Saito. *Physical properties of carbon nanotubes*. World scientific, 1998.
20. Louis, Enrique, et al. "Electron enrichment of zigzag edges in armchair–oriented graphene nano–ribbons increases their stability and induces pinning of the fermi level." *Carbon* 154 (2019): 211-218.
21. Zeng, Hong-Li, et al. "Armchair graphene nanoribbon-based spin caloritronics." *Physics Letters A* 426 (2022): 127892.
22. Chauhan, Nidhi, et al. "An insight into the state of nanotechnology-based electrochemical biosensors for PCOS detection." *Analytical Biochemistry* 687 (2024): 115412.
23. Norian, Erfan, and Bandar Astinchap. "The effect of an external magnetic field, doping, and bias voltage on the thermoelectric and thermodynamic of S-graphene monolayer." *Materials Science in Semiconductor Processing* 156 (2023): 107307.
24. Khemissi, A., and H. Khalfoun. "The electronic transport properties of armchair carbon nanotubes with single and multiple horizontal boron-nitride lines: Unusual effects of high bias voltage on IV characteristics." *Diamond and Related Materials* 140 (2023): 110436.

